THE
PHYSICAL REVIEW

A journal of experimental and theoretical physics established by E. L. Nichols in 1893

SECOND SERIES, VOL. 154, NO. 1 5 FEBRUARY 1967

Absolute Measurements of Total Cross Sections for the Scattering of Low-Energy Electrons by Atomic and Molecular Oxygen*†

GABRIEL SUNSHINE,‡ BERTRAND B. AUBREY, AND BENJAMIN BEDERSON
Department of Physics, New York University, University Heights, New York, New York
(Received 20 September 1966)

The atom-beam recoil technique has been used to measure absolute total cross sections for the scattering of electrons by atomic and molecular oxygen at 22 energies between 0.5 and 11.3 eV, with additional data obtained up to 100 eV. In this method, a modulated electron beam cross-fires an atom beam, whose attenuation at the modulation frequency is observed. A mechanical chopper is utilized so that both the total atom beam and its scattered component can be measured by the same ac detection and amplification systems. It is therefore possible to determine absolute cross sections without requiring knowledge of the beam detection efficiency or the over-all gain of the amplification system. The angular resolution in the electron polar scattering angle ranges from about 15.6° at 1 eV to 9.6° at 12 eV for O, and from about 18.5° at 1 eV to 11.4° at 12 eV for O_2. Our absolute values for O_2 between 0.5 and 11.3 eV are between 10% and 20% higher than those of Brüche, while the shape of the curve agrees well. The atomic cross sections vary from about 5.3 Å² at 0.5 eV to 8.3 Å² at 11.3 eV, with an estimated error of 20%, except for the 0.5-eV point, which has an error of 30%. These results are in excellent agreement with semiempirical calculations of Cooper and Martin and of Robinson and Geltman, as well as with the polarized-orbitals calculation of Temkin, and the the static central field exchange approximation of Myerscough.

I. INTRODUCTION

THE scattering of low-energy electrons by atomic oxygen has been the subject of many theoretical investigations in recent years. For example, calculations of elastic scattering of electrons by atomic oxygen include those of Klein and Brueckner,[1] Cooper and Martin,[2] and Robinson and Geltman.[3] All these calculations are based upon the assumption that the interaction can be represented by a static potential in the energy range below 10 eV. They differ in the form of the potential chosen and in the values of the parameters describing the potentials. These are semiempirical calculations, and they would seem to be particularly appropriate for atoms whose binding energies for the negative ion are known, since behavior of the unperturbed atom's potential at large distances from the origin can be accurately determined by finding the value of a cutoff parameter which yields the correct negative-ion binding energy.[3a] One difficulty with the employment of potential scattering theory lies in the fact that no well-established criteria exist for determining the range of energies for which the theory is valid. One must, to some extent, rely upon experiment to decide this question.

Temkin[4] first employed the method of polarized orbitals for atomic oxygen. Since this is a calculation made from first principles, it should be expected to be more

* Supported by the Advanced Research Projects Agency, through the U. S. Office of Naval Research, and the Defense Atomic Support Agency, through the U. S. Army Research Office, Durham, North Carolina.

† From part of a thesis submitted by G. Sunshine to the Graduate Faculty of New York University in partial fulfillment of the requirements for the degree of Doctor of Philosophy. For a preliminary report of this work see Abstracts of Fourth International Conference on the Physics of Electronic and Atomic Collisions (Science Bookcrafters, Inc., Hastings, New York, 1965), p. 130.

‡ Present address: Department of Physics, New York Institute of Technology, Old Westbury, New York.

[1] M. M. Klein and K. A. Brueckner, Phys. Rev. **111**, 1115 (1958). The semiempirical approach based partly upon knowledge of the binding energy of O^- was first developed in this paper, as a by-product of the calculation of the photodetachment cross section of O^-. The effective-range formula employed is inappropriate for the low-energy electron-atom problem, however. See Ref. 2 for a discussion of this point.

[2] J. W. Cooper and J. B. Martin, Phys. Rev. **126**, 1462 (1962).

[3] E. J. Robinson and S. Geltman, Phys. Rev. **153**, 4 (1967).

[3a] Recently, V. P. Myerscough has also made a static central field calculation with exchange, for the *s*-phase shift only, for energies between 0 and about 1.5 eV. Her results lie very close to those reported in this paper, where they overlap [Phys. Letters **19**, 121 (1965)].

[4] A. Temkin, Phys. Rev. **107**, 1004 (1957). A general scheme for the *ab initio* calculation of elastic scattering by many-electron atoms has been outlined by Bauer and Browne [E. Bauer and H. N. Browne, in *Proceedings of the Third International Conference on Physics of Electronic and Atomic Collisions* (North-Holland Publishing Company, Amsterdam, 1963)], with results given for O. However, details of this calculation have not been published.

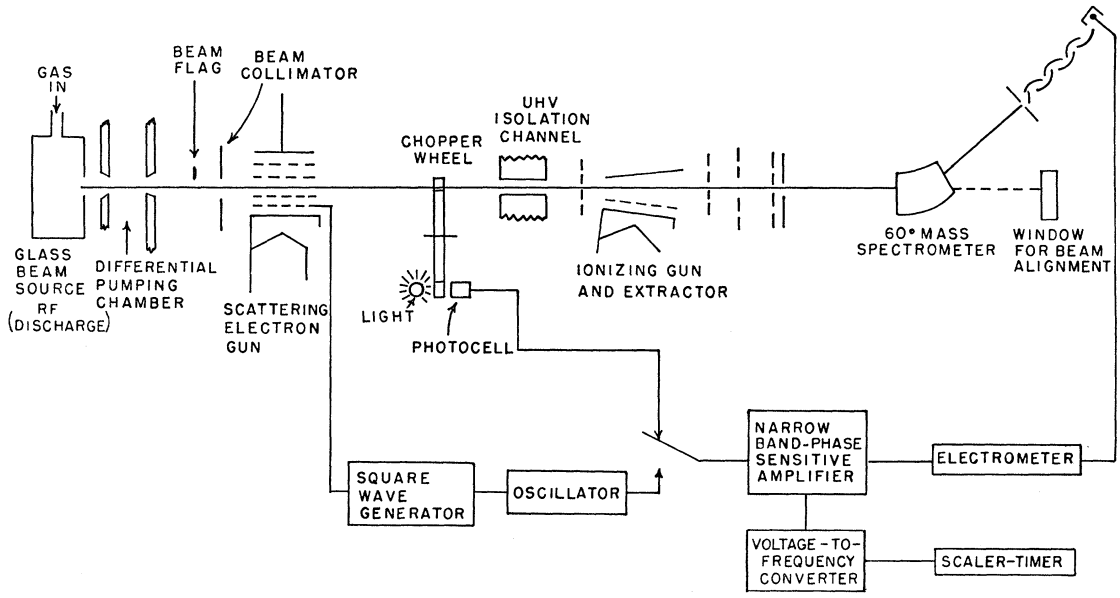

FIG. 1. Schematic diagram of the experimental arrangement.

accurate than potential scattering theory. Of course, such a calculation for atomic oxygen is quite difficult. Temkin's values are in qualitative agreement with those of Refs. 1–3a, although they lie slightly lower (primarily because only *s*-wave scattering was considered). Neynaber *et al.*[5] performed a crossed electron-beam experiment in which the attenuation of the electron beam by the atomic beam was used to obtain relative cross sections which were normalized to the O_2 data of Brüche.[6]

The present experiment employs the atomic-beam recoil method.[7,8] These represent absolute determinations, since the recoil method yields the cross section directly in terms of the electron current, mean beam speed, and certain geometry factors. Knowledge of the atom-beam detection efficiency and of the over-all gain of the electronic system are not required. The results recorded here indicate cross sections relative to O_2 which are larger in the energy range above 6 eV than those of Neynaber *et al.*,[5] but which roughly agree between 2 and 6 eV. The difference at higher energies, however, is about equal to the combined limits of experimental error.

II. EXPERIMENTAL METHOD

A schematic diagram of the experimental arrangement is shown in Fig. 1. The rectangular atomic oxygen beam, which is produced by an rf discharge, is cross-fired by a chopped (50-cps) electron beam. The decrease in atom-beam intensity in the forward direction is observed as an ac signal at 50 cps by the atom-beam detector. The detector is of the "universal" type containing a Weiss-type[9] ionizing gun followed by a magnetic mass spectrometer and electron multiplier. The full beam can be mechanically chopped. This procedure effectively calibrates the detection and electronic systems.

It is shown in the Appendix that the total molecular cross section with the discharge operating is given by

$$Q_m = 1.064(he\alpha_m/i)(S/I), \quad (1)$$

where h is the common dimension of electron and neutral beams in the scattering region, i/e is the electron current (electrons/sec) which passes through the atom beam, α_m is the most probable velocity in the source, and S/I is the ratio of the measured scattering signal to the total beam signal (I is measured using the mechanical chopper). In Eq. (1), corrections have been made for the phase shift at the detector due to the beam transit time from the scattering gun and from the chopper, and also for the fact that both the scattering and detection are density, rather than flux sensitive operations.

The molecular cross section can, of course, be determined either with or without the discharge operating, by setting the mass spectrometer onto the mass-32 peak. [A slightly different numerical coefficient than that of Eq. (1) results if the discharge is off.] Unfortunately, approximately 40% of the mass-16 peak with this discharge operating is produced by dissociative

[5] R. H. Neynaber, L. L. Marino, E. W. Rothe, and S. M. Trujillo, Phys. Rev. **123**, 148 (1961).
[6] E. Brüche, Ann. Physik **83**, 1065 (1927).
[7] K. Rubin, J. Perel, and B. Bederson, Phys. Rev. **117**, 151 (1960).
[8] J. Perel, P. Englander, and B. Bederson, Phys. Rev. **128**, 1148 (1962).
[9] R. Weiss, Rev. Sci. Instr. **32**, 397 (1961).

ionization of O_2.[10] Thus the molecular contribution at the mass-16 position must be subtracted from the total signal to obtain the atomic cross sections. Let R be the ratio of the beam signal at the mass-16 peak to the signal at the mass-32 peak, measured with the discharge off, i.e., R is the production efficiency of O^+ from O_2, relative to that of O_2^+. It is also shown in the Appendix that the atomic cross section Q_a is now given by

$$Q_a=\frac{1.025he\alpha_a}{i}\left(\frac{S_1-RS_2}{I_1-RI_2}\right), \tag{2}$$

where the subscripts 1 and 2 refer to signals recorded at the mass-16 and mass-32 peaks, respectively. All quantities in Eq. (2) are obtained with the discharge operating.

The cross sections as determined from Eqs. (1) and (2) are absolute, in the sense that all quantities are either directly measured (i.e., R, S, I, and i), or are known with reasonable precision (i.e., h, α, and the beam-straggling corrections). On the other hand, the *relative* cross section Q_a/Q_m can be obtained by taking the ratio of Eqs. (1) and (2),

$$Q_a/Q_m=1.362\left[\frac{(I_2S_1/I_1S_2)-R(I_2/I_1)}{1-R}\right]. \tag{3}$$

Here the geometry and mean-speed effects cancel (assuming atoms and molecules possess the same source temperature) leaving only a relatively small beam-straggling correction which is due to the difference in mean beam speeds of O and O_2. Thus, systematic errors are largely eliminated, and it is expected that the error in the ratio Q_a/Q_m will be somewhat smaller than those of the absolute values.

III. APPARATUS

The beam system consists of four adjoining vacuum chambers, separately pumped. These are, first, the source chamber containing the discharge tube, second, a differential chamber, third, the scattering chamber containing the electron-scattering gun and the mechanical chopper, and finally the detector chamber. The detector chamber is an ultrahigh vacuum system, in order to minimize noise due to detection of background gases. During beam operation, typical pressures are 6×10^{-5} Torr in the source chamber, 4×10^{-6} Torr in the differential pumping chamber, 1.5×10^{-7} Torr in the scattering chamber, and 3×10^{-9} Torr in the detector chamber.

Atom-Beam Source

The atomic oxygen source is a low-power rf discharge. The discharge tube is quartz and has an over-all length of 10 cm. Molecular oxygen is mixed with approximately 35% hydrogen to promote dissociation and, typically, 25% dissociation is achieved. The discharge is operated at about 30 Mc/sec and 1.25 Torr, at which pressure the beam can be reasonably well expected to possess a (modified) Maxwellian velocity distribution. The source slit is 0.125 in. high and 0.007 in. wide.

As in the experiment of Neynaber *et al.*, it does not appear likely that a significant fraction of excited-state atomic or molecular species reached the interaction region.[11] This was confirmed for O_2 by the fact that there was no significant difference in the measured O_2 cross sections with and without the discharge operating. Recently, Brink[12] has been unable to observe any metastable ^1S or ^1D atomic oxygen in a beam produced by an rf discharge similar to ours in a magnetic-resonance atomic-beam experiment.

Electron Gun

The scattering gun is a six-electrode structure supported from above by a water-cooled vacuum-chamber flange. It produces a uniform electron beam 0.125 in. $\times$1.500 in. in cross section. Two Alnico bar magnets, positioned outside the vacuum envelope, produce a reasonably uniform magnetic field of about 1000 G, along the electron path.

Retarding potential curves and an analysis of the experimentally observed peak at 2.3 eV in the molecular nitrogen cross section indicate an electron-energy spread of approximately 0.7 eV full width at half-maximum (FWHM) over the energy range of the experiment. (Typical currents employed were of the order of 1 mA.) Two grids and a channel defining the atom-beam height, all kept at ground potential, surround the scattering region to both minimize space-charge effects and prevent stray electric fields from penetrating into the interaction region. The cathode potential is adjusted to provide the desired electron energy. In addition to the second grounded grid, the electrons are collected by a suppressor grid and plate which are both kept at a potential of 40 V positive with respect to ground. This prevents any secondary electrons from reentering the scattering region.

Detection System

Construction details of the Weiss-type ionizing gun used in this experiment are given by Aberth.[13] The length of the electron beam along the atom-beam

[10] See, for example, D. Rapp and P. Englander-Golden, J. Chem. Phys. 43, 1464 (1965). The Weiss ionizing gun produces a deep space-charge trough which traps the positive ions and directs them towards the entrance aperture of the mass spectrometer. This trough is deep enough to trap the O^+ fragments despite their average kinetic energy of several volts.

[11] See, for example, J. W. Linnett and D. G. H. Marsden, Proc. Roy. Soc. (London) A234, 489 (1956).

[12] G. Brink (private communication). However, he has recently observed excited states of both O and O_2, using a high-power (~50-W) microwave discharge [Cornell Aeronautical Laboratory Report No. RM-2156-P-1, 1966 (unpublished)].

[13] W. Aberth, Rev. Sci. Instr. 34, 928 (1963). Also, W. Aberth, G. Sunshine, and B. Bederson, in *Proceedings of Third International Conference on the Physics of Electronic and Atomic Collisions* (North-Holland Publishing Company, Amsterdam, 1963), p. 53.

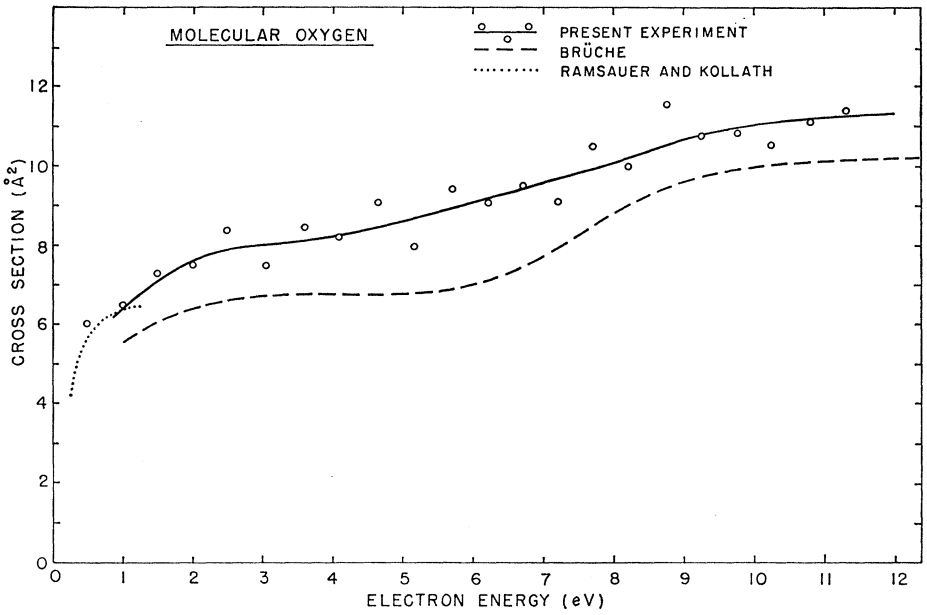

FIG. 2. Total cross section for scattering of electrons by O_2 in the energy range 0.5–11.3 eV. The solid line represents a best smooth-curve fit to the present measurements. The dashed and dotted lines refer to the early measurements of Brüche (Ref. 6) and Ramsauer and Kollath (Ref. 15), respectively.

direction is 1.5 in., and the width is 0.175 in. Typically, about 80 V was applied to the grid and anode, and about 100 mA of useful current was obtained. Extraction electrodes direct the ion current into a 60°-sector-type magnetic analyzer. The detection chamber is bakable and pumped by an Ultek 100-liter/sec ion pump, and is connected to the beam system by a channel with cross-sectional area 0.040 in.×0.4 in. The channel serves the purpose of isolating the ultrahigh vacuum of the detector chamber from the rest of the beam system.

A phase-sensitive lock-in amplifier, synchronized by the ac scattering-gun voltage, was used to detect the ac scattering signal. The dc output of the lock-in was then fed to a voltage-to-frequency converter and then to a scaler-timer for integration.

TABLE I. Molecular (Q_m) and atomic (Q_a) total scattering cross-section data for oxygen.

Electron energy (eV)	Q_m (10^{-16} cm²)	Q_a (10^{-16} cm²)	Q_a/Q_m
11.3	11.4	7.3	0.64
10.8	11.0	8.2	0.72
10.25	10.5	9.5	0.84
9.75	10.7	8.6	0.77
9.25	10.7	8.2	0.75
8.75	11.6	10.1	0.95
8.2	9.9	9.4	0.92
7.7	10.5	8.9	0.81
7.2	9.1	9.1	0.97
6.7	9.5	8.7	0.97
6.2	9.1	6.9	0.81
5.7	9.4	6.3	0.77
5.15	7.9	8.6	1.09
4.65	9.1	6.3	0.80
4.1	8.2	7.6	0.97
3.6	8.5	8.3	1.06
3.05	7.5	6.3	0.81
2.5	8.4	7.9	1.04
2.0	7.5	5.3	0.71
1.5	7.3	6.7	0.93
1.0	6.4	5.2	0.77
0.5	6.0	5.7	0.98

Angular Resolution

The angular resolving power, referred to the *atomic* beam, can be estimated by using the so-called "50% criterion," i.e., the atomic angular resolution; β_0 is defined as being that angle for which 50% of all scattering events are observable by the atom-beam detector.[14] To estimate this quantity we first assume a rectangular beam of infinite height and effective half-width $b=0.028$ in., and a detector of equal half-width. This corresponds, in the Kusch analysis, to the ratio of detector width to beam width equal to unity. The quantity $\rho_0=l\beta_0/b$, where l is the distance from the scattering region to the detector, is then calculated using Eq. (3a) of Ref. 14 to be $\rho_0=1.57$. Since $l=42.1$ in., $\beta_0\simeq10^{-3}$ rad. The resolution is not significantly altered by taking into account the finite beam height, since the ratio of beam height to width is greater than 10. Transforming to the electron polar scattering angle, one finds $\theta_0(V)=(2MV\beta_0/mv)^{1/2}$, where mv and MV are the initial electron and atom momenta, respectively, and we have assumed $mv\ll MV$. It is this assumption which makes β_0 independent of the electron azimuthal scattering angle. The angular resolution referred to the electron polar scattering angle is a function of atom velocity. We obtain an effective resolution by averaging over the velocity distribution of the atom beam to obtain $\langle\theta_0\rangle=(32MkT/\pi m^2v^2)^{1/4}\beta_0^{1/2}$. Using this formula, we calculate the effective angular resolution for atomic oxygen to range from 15.6° at 1 eV to 9.6° at 12 eV, and

[14] P. Kusch, J. Chem. Phys. 40, 1 (1964).

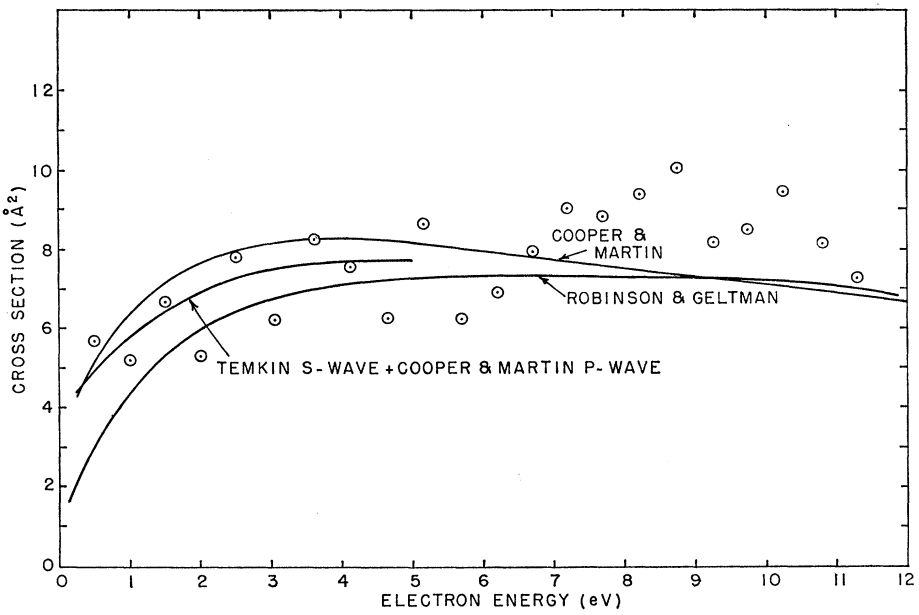

FIG. 3. Total cross sections for scattering of electrons by O, in the energy range 0.5–11.3 eV. The data points are compared to calculations of Cooper and Martin (Ref. 2), Robinson and Geltman (Ref. 3), and Temkin (Ref. 4). The p-wave partial cross section of Cooper and Martin has been added to the s-wave calculation of Temkin.

for molecular oxygen to range from 18.5° at 1 eV to 11.4° at 12 eV. This assumes a beam temperature of 450°K.

IV. DATA AND EXPERIMENTAL ERROR

At each energy, the molecular and atomic scattering signals were usually counted for 4 and 8 min, respectively, and the total molecular and atomic signals (using the mechanical chopper) were counted for 0.2 min. About 125 runs for atomic oxygen were made at 22 energies between 0.5 and 11.3 eV, over a period of several months. Two molecular runs were always taken to bracket each atomic run. The data presented in Table I represent the combined averages of all of these runs. The measured absolute total cross sections for O and O_2, obtained using the parameters of Table II and Eqs. (1) and (2), are given in columns 2 and 3. The ratios Q_a/Q_m are given in column 4. These values represent the averages at each energy obtained by using corresponding pairs of S_1/I_1 and S_2/I_2 in Eq. (3).

The O_2 data are plotted in Fig. 2, along with the results of Brüche[6] and Ramsauer and Kollath,[15] both obtained using a Ramsauer-type apparatus. The curve drawn through our data points represents a modified straight-line least-squares fit.[16] The curvature was estimated by averaging the deviations of adjacent data points from the straight line and by then drawing a smooth curve through these averages. The curve deviates by less than 6% from the least-squares straight line over the entire range of measurements. The shape of the curve agrees quite closely to that of Brüche. Our values are between 10 and 20% higher than the Brüche results, although they agree very well with the Ramsauer-Kollath values over the limited range of overlap. The atomic data points are plotted in Fig. 3, along with the results of several recent calculations. The ratios Q_a/Q_m are given in Fig. 4.

Additional measurements of both O and O_2 were made in the energy range 12–100 eV. The results are plotted in Fig. 5, along with Brüche's O_2 curve, which extends only up to 49 V. Here only two atomic runs were made at each energy. However, the statistics were somehwat better than in the low-energy measurements, because of the higher scattering currents. There is no other experimental or theoretical information concerning atomic oxygen in this energy range.

The principle sources of error in this work are probably systematic in origin. The over-all random error, due primarily to beam noise, is about 10%. The noise arises from fluctuations in source pressure and scattering by background gas, and was about 10 times higher than the shot noise of the beam. A partial list of possible sources of systematic error includes uncertainties in measurement of the apparatus parameters, particularly in h (the common dimension of the interaction region) and in the beam temperature. Long-term drifts in beam temperature, and other long-term variations in apparatus parameters over the course of a given set of molecular and atomic runs, also introduce errors; these, however, are not necessarily systematic when averaged over many sets of runs. The principal errors introduced by the electron gun include errors in the calculated space charge and measured contact-potential corrections to the electron energy during a run, errors in electron path-length due to focusing and to the

[15] C. Ramsauer and R. Kollath, Ann. Physik 4, 91 (1930).
[16] The equation of the least-squares straight line is

$$Q_m = 7.24 + 0.136 V_e,$$

where V_e is the electron energy in eV.

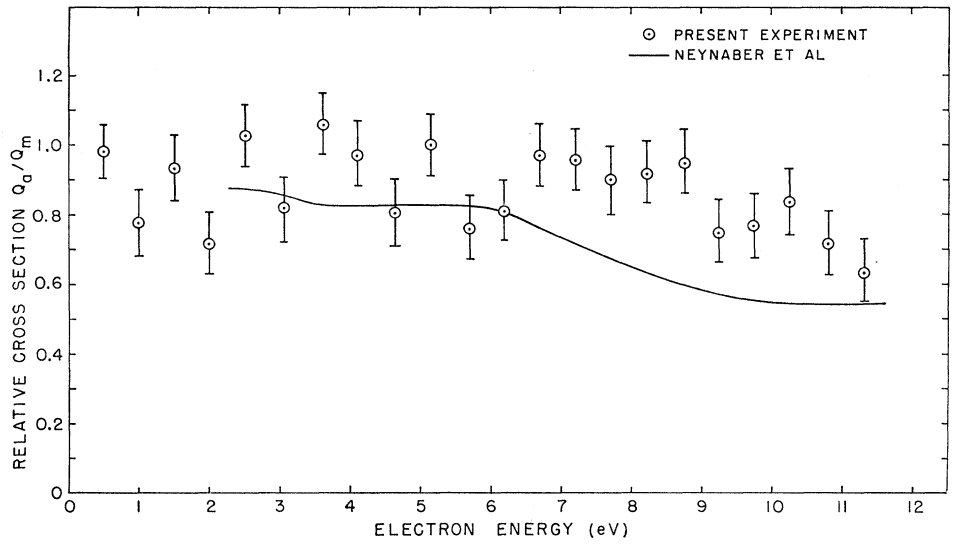

FIG. 4. Comparison of the measured ratios of the atomic to the molecular cross sections Q_a/Q_m, of the present work (circles) to those of Neynaber *et al.* (Ref. 5) (solid line).

helicity effect of the magnetic field, and to reflections of electrons from grids and surfaces. The helicity effect, while calculable in principle, is difficult to estimate accurately, and has not been corrected for in this work. Electron-gun errors are the same for a given set of atomic and molecular runs, so that they do not contribute to the estimated error in the ratio determination.

Our estimate of the over-all systematic error is 18%, and we therefore claim a total error of 20% for the absolute data, with the exception of the 0.5-eV point, for which the error is 30%. The error in the ratio data is 13%, arising from the random errors of 8% and 10% in the molecular and atomic data, respectively.

V. DISCUSSION OF RESULTS

The proper method of comparison of our measurements with those of Neynaber *et al.*[5] is by means of the ratios Q_a/Q_m, since the latter group performed relative measurements normalized to Brüche's molecular curve at each energy. Our molecular cross sections are somewhat higher than those of Brüche, so that a direct comparison of the atomic cross sections would have introduced a systematic bias between the two experiments. In Fig. 4 it is seen that the agreement is reasonably good at energies up to about 6 eV, and that our ratios are somewhat higher than those of Neynaber *et al.* above 6 eV. It should be noted that in this latter energy range the angular resolution in the present work averages to be about 11° in the electron polar scattering angle, while it is about 25° in the Neynaber experiment. A difference in the differential cross section for O and O_2 in this range of scattering angles could account for the discrepancy.

The systematic difference between our O_2 measurements and those of Brüche lies well within the estimated combined systematic errors of both experiments. On the other hand, our measurements at 1 and 0.5 eV are in virtually exact agreement with Ramsauer-Kollath. Clearly more work is required using both crossed-beam and beam-gas techniques, in order to resolve differences in absolute values which are of the order of 20%.[17]

Our atomic data are compared in Fig. 3 with the total elastic cross-section calculations of Cooper and Martin,[2] Robinson and Geltman,[3] and Temkin.[4] The original polarized orbital calculation of Temkin was for *s*-wave scattering only. For a better comparison with experiment, Temkin's curve in Fig. 3 includes the *p*-wave partial cross section calculated by Cooper and Martin. Our results below 7 eV essentially bracket the Robinson-Geltman and modified Temkin calculations (the latter performed only up to 5 eV). Between 7 and 12 eV the Cooper-Martin and Robinson-Geltman calculations are virtually identical and lie slightly below the average of our data points. The difference here could readily

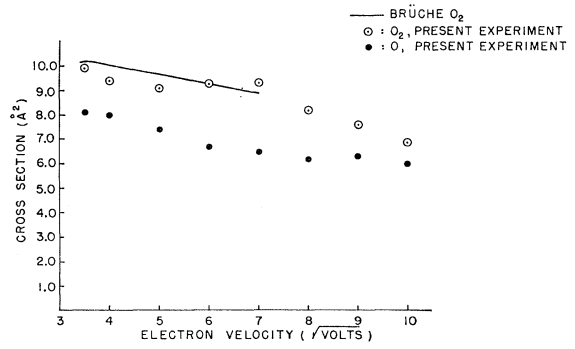

FIG. 5. Total cross sections for scattering of electrons by O and O_2 in the energy range 12–100 eV. The solid curve represents the O_2 measurements of Brüche (Ref. 6).

[17] Some of the difficulties in absolute cross-section determinations are discussed in a critical review of ionization cross sections by Kieffer and Dunn [L. J. Kieffer and G. H. Dunn, Rev. Mod. Phys. 38, 1 (1966)]. Many of the problems discussed therein apply equally to total cross-section measurements.

be accounted for by the contribution of inelastic channels to the total (measured) cross section.

The agreement of experiment with semiempirical potential scattering theory, on the one hand, and with a quasidynamic calculation made from first principles, on the other hand, is therefore seen to be extremely good in the "low-" energy domain.

ACKNOWLEDGMENTS

Dr. William Aberth performed a large part of the design and construction of the apparatus, and participated in some of the early work on O_2. We wish to thank Dr. E. Robinson and Dr. S. Geltman for some enlightening conversations. One of us (G.S.) gratefully acknowledges support by NASA.

APPENDIX

In a molecular beam which is formed by effusion, the beam intensity, $J(v)dv$, from particles with velocities between v and $v+dv$ is

$$J(v)=(2J_0v^3/\alpha^4)\exp(-v^2/\alpha^2), \quad \text{(A1)}$$

where J_0 is the full beam intensity and $\alpha\equiv(2kT/m)^{1/2}$ is the most probable velocity in the source. In the present experiment the beam was detected by an electron-bombardment ionizer in which the probability that a particle is ionized is proportional to the time spent in the detector, i.e., inversely proportional to the velocity of the particle. Therefore, the velocity distribution in the detected beam is

$$J_i(v)=(2J_0B_iv^2/\alpha^4)\exp(-v^2/\alpha^2), \quad \text{(A2)}$$

where B_i/v is the probability that a beam particle with velocity v is detected. Similarly, the velocity distribution in the beam which is first scattered and then detected is

$$J_s(v)=(2J_0B_iB_sv/\alpha^4)\exp(-v^2/\alpha^2), \quad \text{(A3)}$$

where (B_s/v) is the probability that a beam particle with velocity v is scattered. The collision cross section Q and B_s are related by the expression

$$B_s=Qi/he, \quad \text{(A4)}$$

where i/e is the electron-scattering current in electrons per second and h is the common electron and atom beam heights in the interaction region.

There is still a further factor to be introduced in the distribution of detected velocities in the beam when phase-sensitive detection is used. The output of the electronics gives a signal proportional to the input signal multiplied by the cosine of the phase angle between it and an arbitrary phase reference signal. Since a beam particle requires a time l/v to travel the distance l from the modulation region to the detector, it is seen that the output signal of the phase-sensitive detection system is

$$J_i=\frac{2J_0B_iG_i}{\alpha^4}\int_0^\infty v^2\cos[\phi_2+(2\pi\nu l_2/v)]\times\exp(-v^2/\alpha^2)dv, \quad \text{(A5)}$$

when the full beam is detected, and

$$J_s=\frac{2J_0B_iB_sG_s}{\alpha^4}\int_0^\infty v\cos[\phi_1+(2\pi\nu l_1/v)]\times\exp(-v^2/\alpha^2)dv, \quad \text{(A6)}$$

when the scattered beam is detected. In the above, l_2 is the distance from the beam chopper to the detector, l_1 is the distance from the electron scattering gun to the detector, ν is the modulation frequency, ϕ_1 and ϕ_2 are the arbitrary phase angles which depend upon the setting of a phase-shift control in the electronics, and G_i and G_s are determined by the gain control on the electronics.

Equation (A5) can be written as

$$J_i=\frac{2J_0B_iG_i}{\alpha}[I_2(x_2)\cos\phi_2-K_2(x_2)\sin\phi_2] \quad \text{(A7)}$$

and Eq. (A6) can be written as

$$J_s=\frac{2J_0B_iB_sG_s}{\alpha^2}[I_1(x_1)\cos\phi_1-K_1(x_1)\sin\phi_1], \quad \text{(A8)}$$

where

$$I_n(x_n)\equiv\int_0^\infty y^n\cos(x_n/y)\exp(-y^2)dy, \quad \text{(A9)}$$

and

$$K_n(x_n)\equiv\int_0^\infty y^n\sin(x_n/y)\exp(-y^2)dy. \quad \text{(A10)}$$

Here $x_n\equiv 2\pi\nu l_n/\alpha$, and the index n takes on the values 1 and 2. The general problem of velocity dispersion of square-modulated beams has been discussed by Harrison, Hummer and Fite.[18] They have evaluated and tabulated the integrals (A9) and (A10) for $2\leqslant n\leqslant 5$ and $0\leqslant x\leqslant 20$. The values of the integrals $I_1(x)$ and $K_1(x)$ were calculated in the present work using the recursion relations

$$I_{n-1}(x)=\frac{1}{x}[(n+1)K_n(x)-2K_{n+2}(x)]$$

and

$$K_{n-1}(x)=\frac{1}{x}[2I_{n+2}(x)-(n+1)I_n(x)],$$

and the values $I_2(x)$, $I_4(x)$, $K_2(x)$, and $K_4(x)$ of Harrison *et al.*

[18] H. Harrison, D. G. Hummer, and W. L. Fite, Boeing Scientific Laboratories Flight Sciences Laboratory, Technical Memorandum No. 26, 1964 (unpublished).

TABLE II. Apparatus parameters.

α_a	(most probable oven velocity of atomic oxygen, $T=450°K)=6.85\times10^4$ cm/sec
α_m	(most probable oven velocity of molecular oxygen, $T=450°K)=4.84\times10^4$ cm/sec
l_1	(distance from scattering region to detector) = 104.0 cm
l_2	(distance from mechanical chopper to detector) = 58.5 cm
ν	(electron and mechanical chopping frequency) = 50 cps

In the experiment described here, full-beam and scattering signals were obtained with the discharge on for both mass 32 and mass 16. The mass-32 signals were due only to the molecular oxygen in the beam. Therefore, Eqs. (A7) and (A8) can be used without modification to obtain the molecular-oxygen cross section. Let J_m equal the molecular component of the full-beam intensity, and let I_m and S_m equal the normalized mass-32 full-beam and scattering signals, respectively, at the output of the phase-sensitive detection system. Then Eqs. (A7) and (A8) for the mass-32 signals are

$$I_m=\frac{2J_mB_{mi}}{\alpha_m}[I_2(x_{2m})\cos\phi_2-K_2(x_{2m})\sin\phi_2], \quad \text{(A11)}$$

and

$$S_m=\frac{2J_mB_{mi}B_{ms}}{\alpha_m^2}[I_1(x_{1m})\cos\phi_1-K_1(x_{1m})\sin\phi_1]. \quad \text{(A12)}$$

Solving these equations for B_{ms} gives

$$B_{ms}=\frac{\alpha_mS_m}{I_m}\left[\frac{I_2(x_{2m})\cos\phi_2-K_2(x_{2m})\sin\phi_2}{I_1(x_{1m})\cos\phi_1-K_1(x_{1m})\sin\phi_1}\right]. \quad \text{(A13)}$$

The adjustable phase angles ϕ_2 and ϕ_1 were set to maximize the signals I_m and S_m. This is equivalent to setting $\partial I_m/\partial\phi=0$, and $\partial S_m/\partial\phi=0$. Therefore,

$$\phi_2=-\tan^{-1}[K_2(x_{2m})/I_2(x_{2m})], \quad \text{(A14)}$$

and

$$\phi_1=-\tan^{-1}[K_1(x_{1m})/I_1(x_{1m})]. \quad \text{(A15)}$$

TABLE III. Calculated values of $I_n(x)$, $K_n(x)$, and ϕ_n.

	$I_1(x)$	$K_1(x)$	$I_2(x)$	$K_2(n)$	ϕ
$X_{2a}=0.27$	...	...	0.41574	0.12607	$\phi_2=-23.5°$
$X_{2m}=0.38$	...	...	0.39220	0.17159	
$X_{1a}=0.48$	0.33906	0.26861	...	...	$\phi_1=-52°$
$X_{1m}=0.68$	0.24774	0.31685	...	...	

The mass-16 signals were due to both atomic oxygen in the beam and dissociative ionization of the molecular oxygen in the beam by the detector electron gun. Let J_a be the atomic component of the full-beam intensity, and let I_a and S_a equal the normalized mass-16 full-beam and scattering signals, respectively, at the output of the phase-sensitive detection system. Then, if B_{di}/v is the probability that an oxygen molecule with velocity v undergoes dissociative ionization and is detected, Eqs. (A7) and (A8) for the mass-16 signals are

$$I_a=\frac{2J_aB_{ai}}{\alpha_a}[I_2(x_{2a})\cos\phi_2-K_2(x_{2a})\sin\phi_2]+\frac{2J_mB_{di}}{\alpha_m}\times[I_2(x_{2m})\cos\phi_2-K_2(x_{2m})\sin\phi_2], \quad \text{(A16)}$$

and

$$S_a=\frac{2J_aB_{ai}B_{as}}{\alpha_a^2}[I_1(x_{1a})\cos\phi_1-K_1(x_{1a})\sin\phi_1]+\frac{2J_mB_{di}B_{ms}}{\alpha_m^2}[I_1(x_{1m})\cos\phi_1-K_1(x_{1m})\sin\phi_1]. \quad \text{(A17)}$$

Since I_m and I_a were measured with the same phase setting, and S_m and S_a were also measured with the same phase setting, the phase angles ϕ_2 and ϕ_1 in the above expressions for I_a and S_a are those given by Eqs. (A14) and (A15). Substitution of Eqs. (A11) and (A12) into Eqs. (A16) and (A17) and solving for B_{as} gives

$$B_{as}=\alpha_a\left[\frac{S_a-RS_m}{I_a-RI_m}\right]\times\left[\frac{I_2(x_{2a})\cos\phi_2-K_2(x_{2a})\sin\phi_2}{I_1(x_{1a})\cos\phi_1-K_1(x_{1a})\sin\phi_1}\right], \quad \text{(A18)}$$

where $R\equiv B_{di}/B_{mi}$ is the ratio of the mass-16 full-beam signal to the mass-32 full-beam signal with the discharge off. The appropriate parameters of the present experiment are given in Table II, while the calculated values of $I_n(x)$, $K_n(x)$ and ϕ_n are given in Table III. Using these quantities in Eqs. (A4), (A13), and (A18), we get

$$Q_m=1.064(he\alpha_mS_m/iI_m) \quad \text{(A19)}$$

and

$$Q_a=1.026\frac{he\alpha_a}{i}\left[\frac{S_a-RS_m}{I_a-RI_m}\right]. \quad \text{(A20)}$$